Military Technical College
Kobry El-Kobbah,
Cairo, Egypt.

16th International Conference on Applied Mechanics and Mechanical Engineering.

EFFECT OF BASE BLEED DIMENSIONS ON THE BALLISTIC PERFORMANCE OF ARTILLERY PROJECTILES

H. A. Abou-Elela*, A. Z. Ibrahim*, O. K. Mahmoud* and O. E. Abdel-Hamid*

ABSTRACT

Base bleed unit is one of the active methods to increase the range of artillery projectiles. Ballistic performance of base bleed unit has been experimentally assessed using firing tests and wind tunnel experiments. Meanwhile, analytical and numerical studies have been carried out. In some of these studies, solid propellant is used as the source of the burnt gases ejected into the wake behind the projectile base. But, in other studies, different types of gases such as air, argon, hydrogen, and helium are ejected at different temperatures.

In this paper, the effects of the main dimensions of 2-parts tubular base bleed grain unit on its ballistic performance are studied analytically. These dimensions are base bleed grain maximum radius, length, inner diameter of the grain, and exit diameter of base bleed unit. The study is applied to the base bleed unit which is installed to K307 155mm projectile. The study leads to a new method to control the ejected mass flow rate. This method is based on changing the exit diameter of base bleed unit in order to get higher injection parameter in the first few seconds of projectile flight and lower values in the remaining time of base bleed grain burning. Therefore, the base bleed projectile range is increased by 1.7 % when comparing with its counterpart which is supplied with base bleed unit having constant exit diameter and the same base bleed grain.

KEY WORDS

Aerodynamics, base bleed, range extension, drag reduction.

---

* Egyptian Armed Forces.

INTRODUCTION

Base bleed unit is one of the active methods to increase the range of artillery projectiles. Ejected gases from the base bleed unit are responsible for the base drag reduction resulting in range extension of artillery projectiles. Base bleed effect has been studied by many researchers using different approaches such as firing tests [1-5], wind tunnel experiments [6-9], analytical methods [10-17] and computational fluid dynamic simulations [18- 21]. In some of these studies, the researchers used solid propellants as the source of the ejected gases. Others used different types of hot or cold gases such as air, argon, hydrogen, and helium. These studies focused on the effect of the flow parameters and the base ejection configurations on drag reduction. Base bleed unit which ejects hot gases due to burning of solid propellant is still the mostly applied type. The propellant could be of composite or double base propellant type with low burning rate that is able to burn in a low atmospheric condition resulting from the wake behind the projectile base.

The used configurations of base bleed grain are tubular, slotted tubular cylinder or donut shape. The most common applied one is the slotted tubular cylinder or donut shape. The number of slots is 2 or 3 slots splitting the base bleed grain into 2 or 3 equal parts, respectively. The main dimensions of base bleed grain are the maximum radius (R_{max}), grain length (L_i) and the inner diameter (R_{in}).

In order to maximize the range extension of base bleed projectile, grain dimensions are discussed according to: 1) the required ballistic performance of base bleed, 2) the design constrains for both the projectile body strength of material and its aerodynamics, 3) the maximum pressure inside the barrel affecting projectile base that will have an influence on the mechanical properties required in base bleed grain production and 4) the projectile lethality. It has been proven in Ref. [17] that base drag reduction - via base bleeding - at high supersonic velocities of artillery projectiles is more efficient.

It means that the base bleed unit is of better performance at the first few seconds of projectile flight after its departure the barrel muzzle. Therefore maximum range of base bleed projectile can be obtained when the base bleed grain generates relatively large mass flow rate to get optimum value of the injection parameter value at the first few seconds of projectile flight with supersonic speed [22].

The computational work presented in Ref. [13] showed that the increase in base pressure due to the base bleed unit is proportional to the projectile flying velocity. It means that at the same injection parameter, the higher speed of base bleed projectile, the higher base pressure.

Studying the effect of base bleed grain dimensions on the ballistic performance of artillery projectiles is important in case of providing rocket assisted unit. This requires adapting the working time of each unit by optimizing dimensions of their grains so that no interaction may happen between them to ensure maximum range without massive reduction of projectile lethality.

In this study, the effect of the main dimensions of base bleed grain is discussed through an analytical model which its predictions were previously verified [17]. These

dimensions are the length, inner diameter and maximum diameter. Effect of base bleed exit diameter is also discussed. A new method is presented to control the mass flow rate and consequently the injection parameter by using a deformable exit diameter.

The present study is applied to a base bleed projectile model K307 launched with muzzle velocity 910 m/s at angle of fire 51.2° which corresponds to the maximum range. Base bleed grain consists of two identical solid propellant grains as shown in Fig. 1 [17]. The surfaces exposed to burning are an inner cylinder and four flat surfaces; each pair is separated by a slot (ω_i) of 3 mm. The slots are held opened during launch by four spacers. Other surfaces of the grain are covered by inhibitor.

GOVERNING EQUATIONS OF FLOW RATES AND FLOW REGIMES

The grain should burn out at time equals to nearly the half of projectile time of flight [14]. Experimental work showed that the optimum injection parameter for base bleed projectile is approximately 0.005 [23]. The injection parameter is calculated according to the following equation [17]:

$$I = \frac{\dot{m}_N}{\dot{m}_\infty}, \tag{1}$$

where $\dot{m}_N$ is the mass flow rate of burnt gases through the base bleed nozzle and $\dot{m}_\infty$ is the upstream mass flow rate of air past the projectile base which can be determined using the following equation [17]:

$$\dot{m}_\infty = \rho_\infty V_\infty A_b \tag{2}$$

where ρ_∞, V_∞ are the free stream density and velocity, respectively, A_b is the area of the boattail base. The mass flow rate ($\dot{m}_N$) is a function of the burning rate of base bleed grain composition and the exposed instantaneous grain surface (A_{bb}).

$$\dot{m}_N = U\, A_{bb}\, \rho_{bb}\,, \tag{3}$$

where ρ_{bb} and U are the density and burning rate of the base bleed grain composition, respectively. The grain burning rate can be calculated according to the following equation [2]:

$$U = k\, U_0\, P_{ch}^{\alpha}, \tag{4}$$

where k is the spin rate factor, U_o is the grain burning rate at atmospheric pressure, P_{ch} is the pressure of the base bleed unit chamber and α is the pressure exponent.

Based on the value of mass flow rate [14] (see Fig. 2), there are three regimes of base flow as follows:

Regime I: The base bleed gases provide a part of the mass required for the mixing layer entrainment process which is created between the free stream flow and the primary recirculating region (PRR) which lies behind the projectile base. The strength

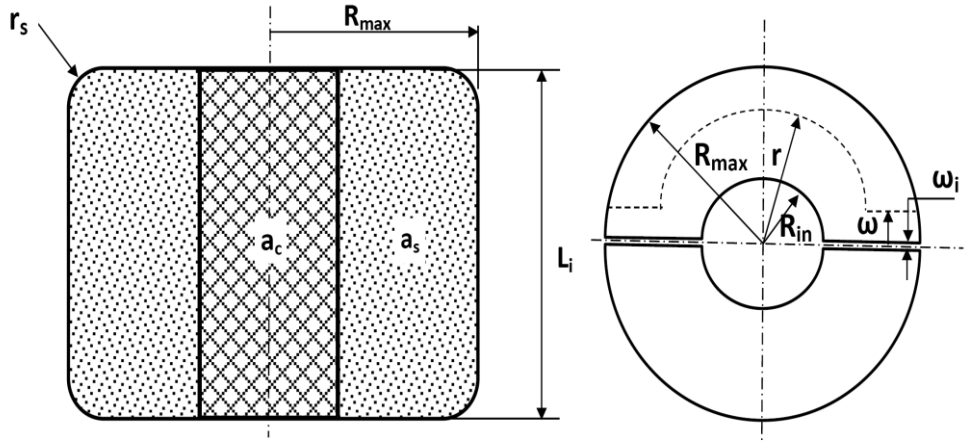

Fig. 1. Geometry of the base bleed grain [17].

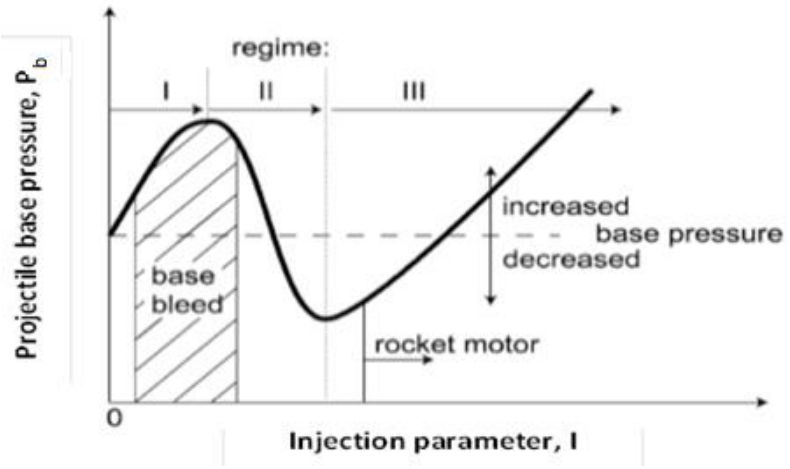

Fig.2. Base pressure versus injected mass flow rate [19].

of PRR decreases with the injection rate and the recompression shock is weakened and consequently increases base pressure.

Regime II: It starts when the injection parameter is sufficient providing gases required by the mixing entrainment process. At this point, the recompression shock is weakened, and the base pressure reaches a maximum value at the optimum value of injection parameter. If the injection parameter exceeds its optimum value, the projectile base pressure decreases until the injected gases have enough momentum to penetrate through the primary recirculation region then the pressure may decrease to a value less than its counterpart without base bleed unit as demonstrated in the experimental work discussed in Ref. [24]. This occurs at the end of the regime

Regime III: It starts when the injection parameter increases even further, and eventually leads to power-on conditions which is not used for base bleed

applications. All the analytical models put into consideration the effect when the injection parameter exceeds the optimum value [15-17].

RESULTS and DISCUSSIONS

In the following, the predicted results due to the application of analytical model of Ref. [17] on the base bleed projectile model K307 are classified into: i) results due to the effect of maximum radius of base bleed grain on range, ii) results due to the effect of grain length on range, iii) results due to the effect of base bleed grain inner radius on range. Finally the effect of exit diameter of base bleed unit is presented.

Effect of Maximum Radius of Base Bleed Grain R_{max}

Figure 3 shows the predicted range and base bleed grain bleeding time versus maximum radius of base bleed grain. It can be noted that the range is linearly increased with R_{max} up to R_{max} = 50 mm. With further increase in R_{max}, the range increases with smaller rate until insignificant increase in range at R_{max} > 60 mm is predicted which seemed to be the optimum radius comparing of the data of the used projectile. For the bleeding time, it increases with the increase of the R_{max} resulting in increasing in the radial thickness of the grain which equals (R_{max} – R_{in}) providing more thickness to burn.

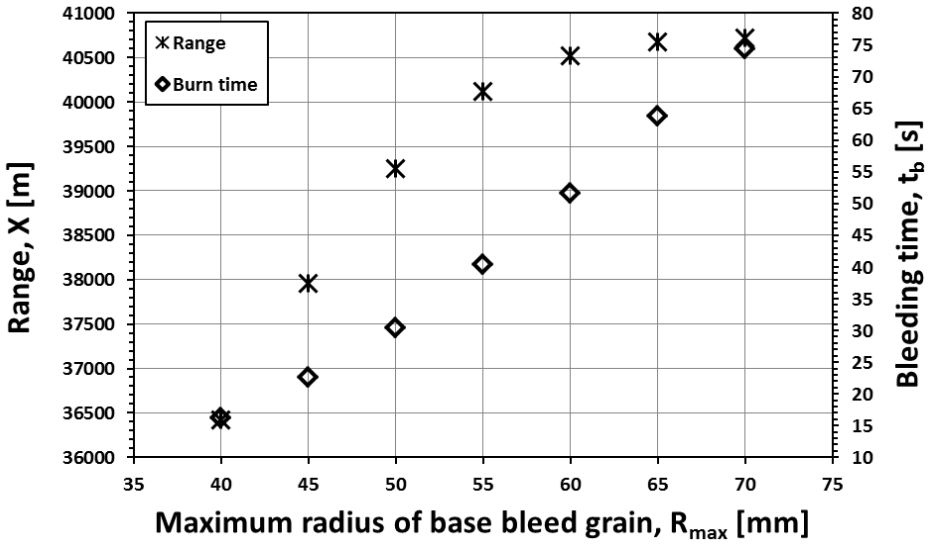

Fig. 3. Predicted range and bleeding time versus maximum radius of base bleed grain.

Figures 4 and 5 display the change of projectile altitude and Mach number with time of flight, respectively, at different values of the grain maximum radius, namely R_{max} =40, 60 and 70mm. It can be noted that there is insignificant change when comparing the altitude or the Mach number at R_{max}=60 and 70 mm. Also from figures 3 and 4 it is clear that the bleeding time of base bleed grain of radius = 40 and 60 mm finished at the ascending part of projectile trajectory but for the radius = 70 mm the bleeding time continued in the descending part.

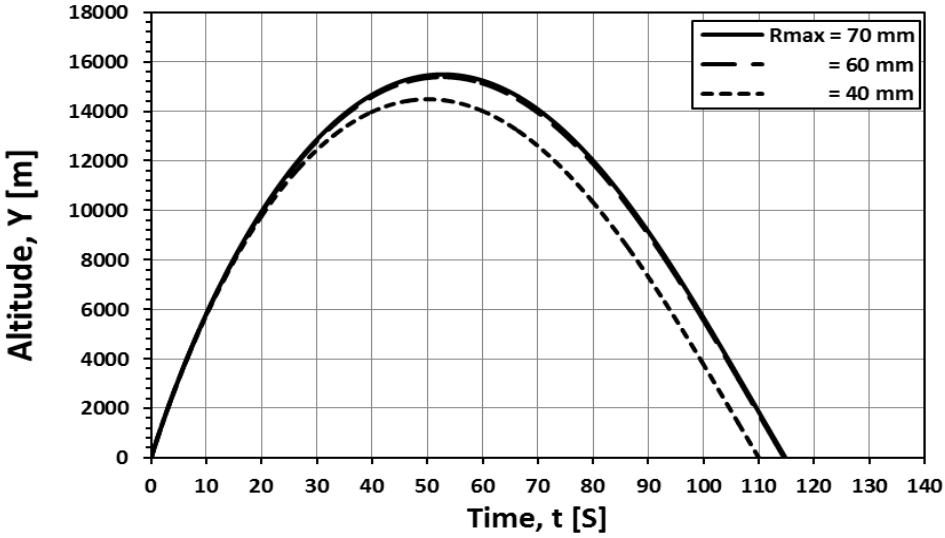

Fig. 4. Predicted change of projectile altitude versus time of flight for different maximum radii of base bleed grain.

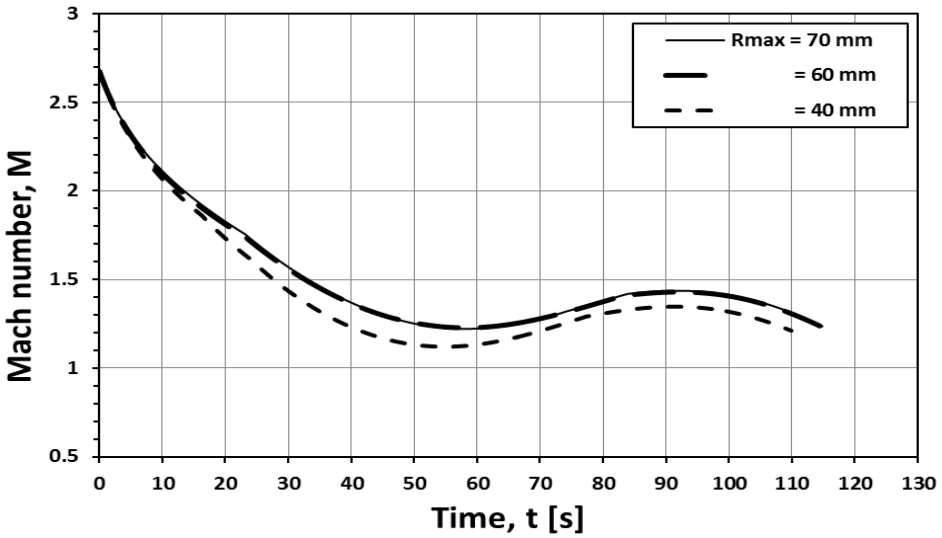

Fig. 5. Predicted change of projectile Mach number versus time of flight for different maximum radii of base bleed grain.

Figure 6 plots the change of base bleed grain surface areas (slots – cylindrical- total) and grain length with bleeding time for three values of R_{max}. For each R_{max}, the figure shows that the area of slots decreases but the cylindrical area increases with bleeding time. The rate of decreasing the slot area is approximately the same as the rate of increasing the cylindrical area. Therefore, the change of total area is slightly decreasing with bleeding time. When increasing R_{max}, the slots burnt surface area increases, the cylindrical area for the same bleeding time is the same for all values of R_{max} up to the time corresponds to radius of burn equals to value $r = R_{max} - r_s$ which is identified by the point at which the grain length starts to decrease under the effect of the radius of curved ends of the grain, r_s (see Fig. 1). However, higher value of R_{max} will provide more radial thickness to burn and consequently increases the cylindrical and total areas as whole.

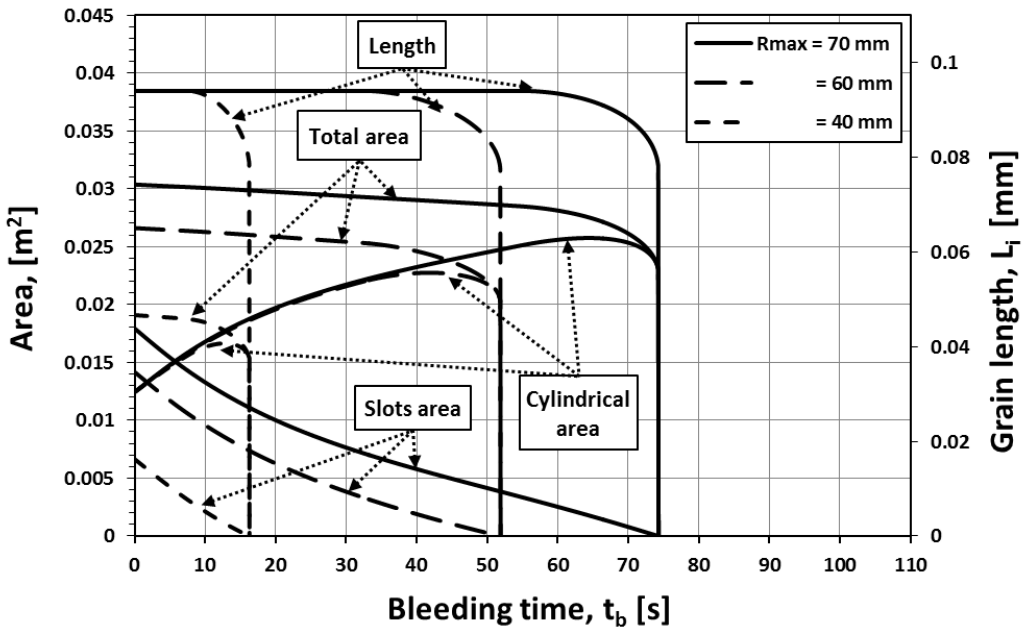

Fig. 6. Change of base bleed grain surface areas (cylindrical – slots- total) and grain length with bleeding time at different maximum radii of base bleed grain.

Figure 7 plots the predicted change of mass flow rate and the injection parameter with bleeding time for three value of R_{max}. It can be noted from this figure that the mass flow rate as well as the injection parameter increase by the increase of R_{max} at the same burning rate of base bleed grain composition. This is mathematically proofed when referring to Eq.3 since A_{bb} is proportional to R_{max}.

When studying the trend of the mass flow rate at a specified value of R_{max}, it is clear that the mass flow rate increases for about 2 seconds with average percentage 4% and then decreases with time. This compiles with the published for base bleed projectile model M864 in Ref. [13]. It is though the reason of this trend is that during the 2 seconds the change in base bleed burnt area and the same for free stream velocity and pressure is negligible. The high mass flow rate that is generated at time = 0 leads to high chamber pressure, base pressure, burn rate as shown in the next figures, and consequently increases mass flow rate. This is true till the reduction in free stream conditions and base bleed burnt area become dominate during the ascending part of projectile flight, so chamber pressure decreases and consequently mass flow rate decreases. The mass flow rate decreases with bleeding time as a result of the decreasing the total area of the base bleed grain as shown previously and due to the continuous decrease of the free stream pressure during the ascending part of the projectile trajectory. For R_{max} =70 mm, the mass flow rate increases after the time moment when t = 53 s which corresponds to the time of the trajectory apex hence the free stream pressure increases in a portion of the descending part of projectile trajectory (see Figures 3 and 4). However mass flow rate in general decreases with time but the injection parameter increases since the free stream conditions represented by velocity and density decrease with time of projectile flight in the ascending part of trajectory (see Eqs.1, 2).

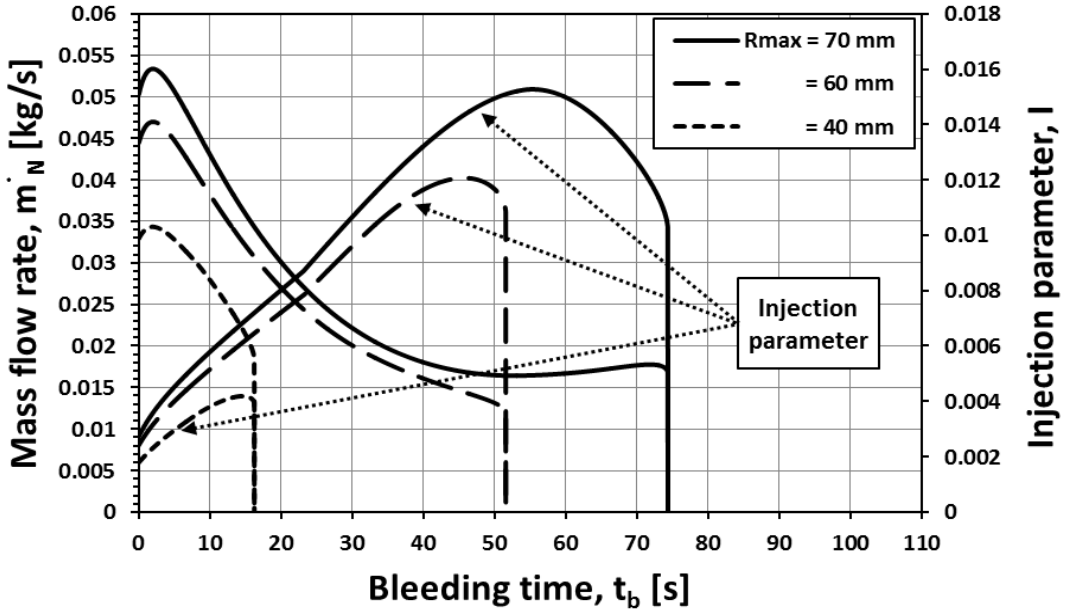

Fig. 7. Predicted change of mass flow rate and the injection parameter with of projectile flight for different maximum radii of base bleed grain.

Figure 8 depicts the change of the pressure behind the projectile base with time of projectile flight for the different values of R_{max}. With the increase in R_{max}, the projectile base pressure slightly increases. Thus, the base drag decreases and consequently the projectile range increases. The sudden drop of the base pressure value corresponds to the moment of end of burn at which is assumed that the chamber pressure equals to the base pressure [11-17]. In the remaining time of projectile flight in case of R_{max} = 40 mm, the base pressure is the highest because the projectile takes the lowest trajectory (see Fig. 4). However for R_{max} = 70 mm the increase in base pressure becomes insignificant as the injection parameter values in more points during the time of base bleed grain burn exceeds the optimum value and this explains the trend shown in Fig.3.

Effect of Length of Base Bleed Grain (L_i)

Figure 9 shows the change of projectile range and base bleed grain bleeding time versus base bleed grain length. The range increases with the increase of the length up to L_i = 110 mm then, the range decreases. The bleeding time continuously decreases with the increase of L_i. This result is agreed with that reported in Ref. [14].

Figure 10 displays the predicted projectile altitude versus time of flight at different values of the grain length namely L_i=65, 85, 110, 150mm. It can be noted that the maximum altitude is obtained by increasing L_i up to a certain value then it decreases.

Figure 11 plots the predicted projectile Mach number with the projectile time of flight for the selected values of the grain length. Mach number and projectile time of flight increase with the increase of grain length up to L_i = 110 mm. In case of L_i = 150 mm, the Mach number values are the highest up to time = 23 seconds then started to

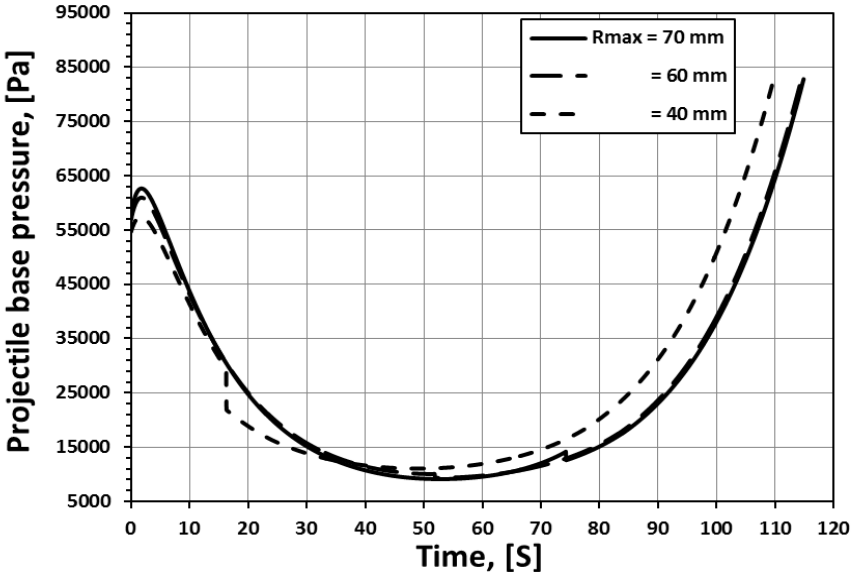

Fig. 8. Change of the pressure behind the projectile base with time of projecti flight for different maximum radii of base bleed grain.

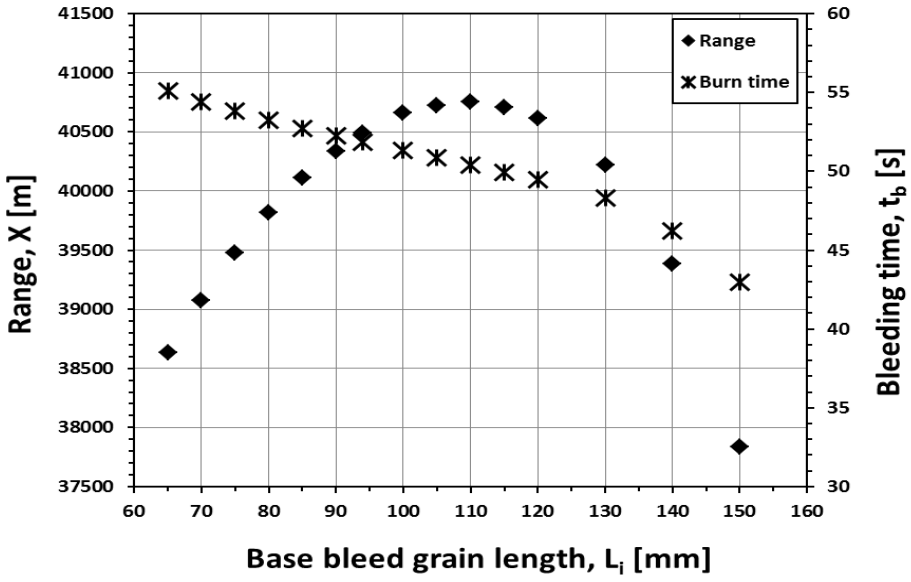

Fig. 9. Change of projectile range and base bleed grain bleeding time versus base bleed grain length.

decrease with higher rate till it becomes the lowest at time = 34 seconds comparing with the corresponding data related to other values of L_i.

Figure 12 plots the change of base bleed grain surface areas (slots – cylindrical-total) with the bleeding time at different L_i. At the specified value of L_i, the trends of the change of surface areas with bleeding time are as the same as shown in case of increasing maximum radius, cf. Fig. 6. However when increasing L_i both cylindrical and slots areas increase and this leads to the increase of total area up to the end of

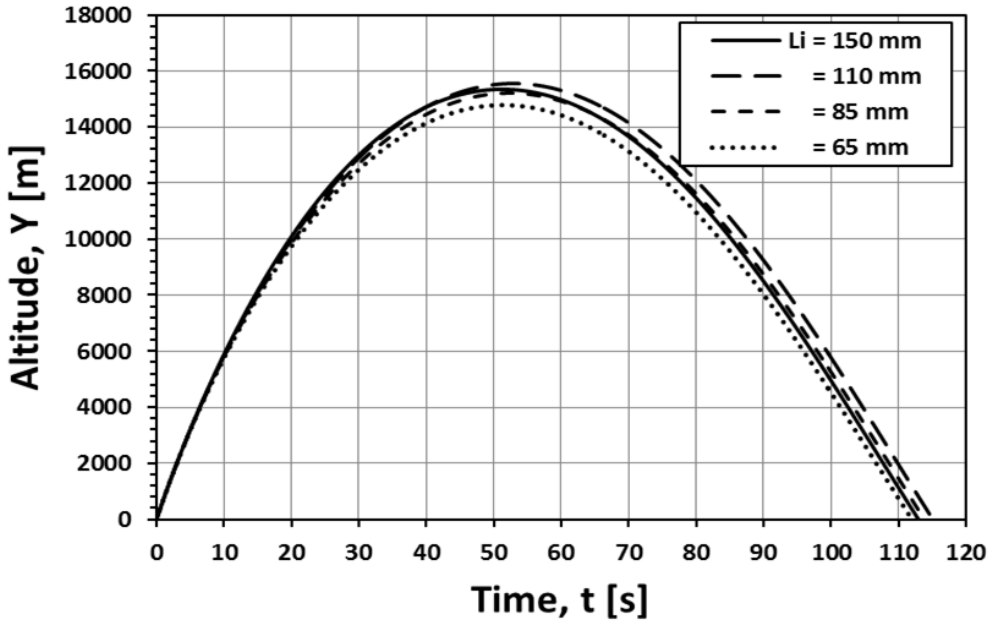

Fig. 10. Predicted change of projectile altitude versus time for different base bleed grain length

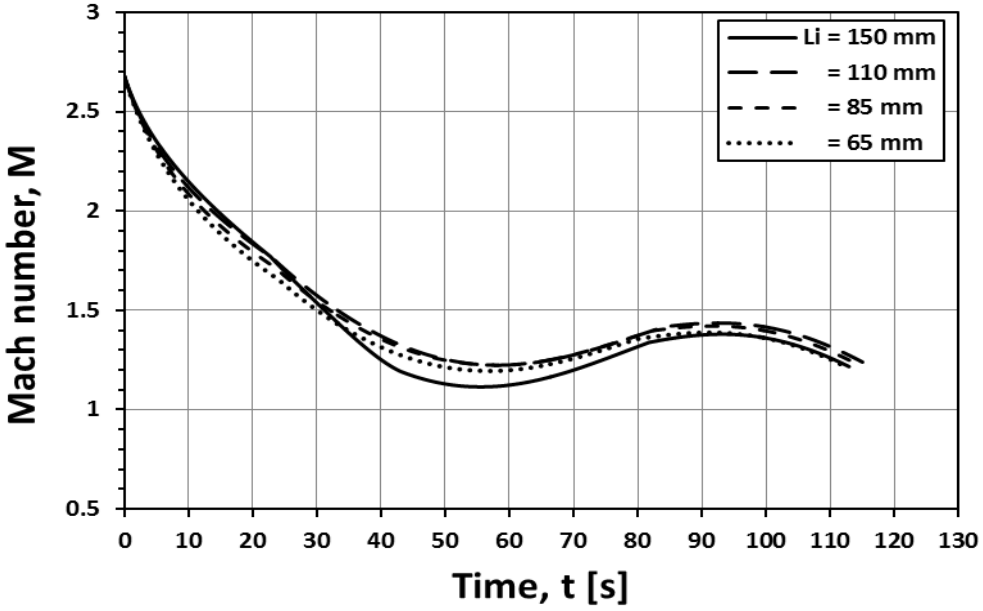

Fig. 11. Change of projectile Mach number versus time of flight for different grain lengths.

bleeding time. The increase in the total area generates more mass flow rate and injection parameter with increasing L_i as shown in Fig. 13. The generation of high mass flow rate with increasing L_i leads to higher pressure in the base bleed chamber up to the end of bleeding time as shown in Fig.14.

In case of different grain dimensions with the same U_0, the factors that influence the time of burning are: 1) grain radial thickness, 2) the burn rate, U which depends on base bleed chamber pressure (see Eq. 4).

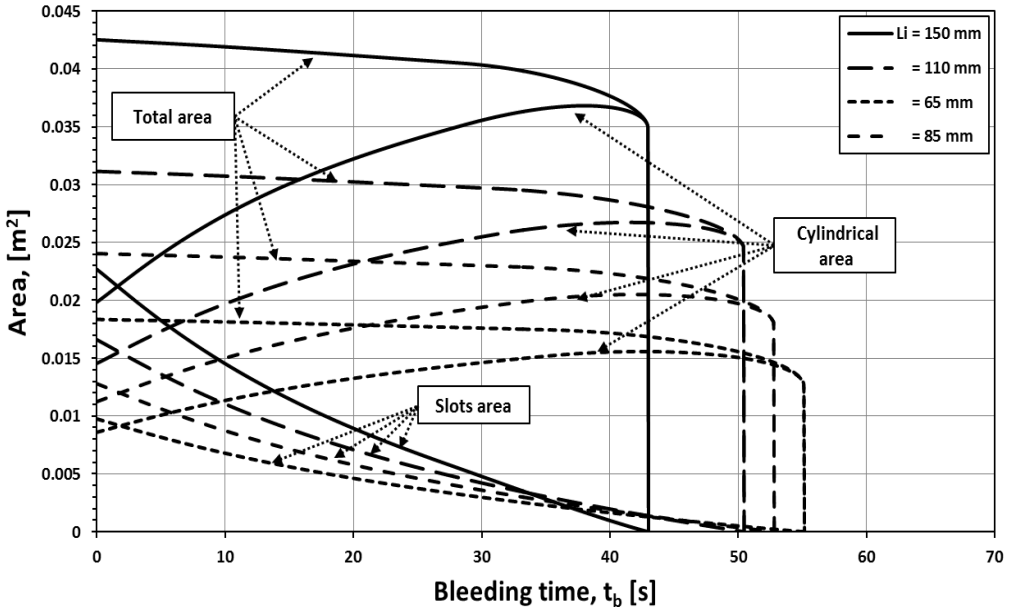

Fig. 12. Change of base bleed grain surface areas (cylindrical – slots- total) with bleeding time for different base bleed grain lengths.

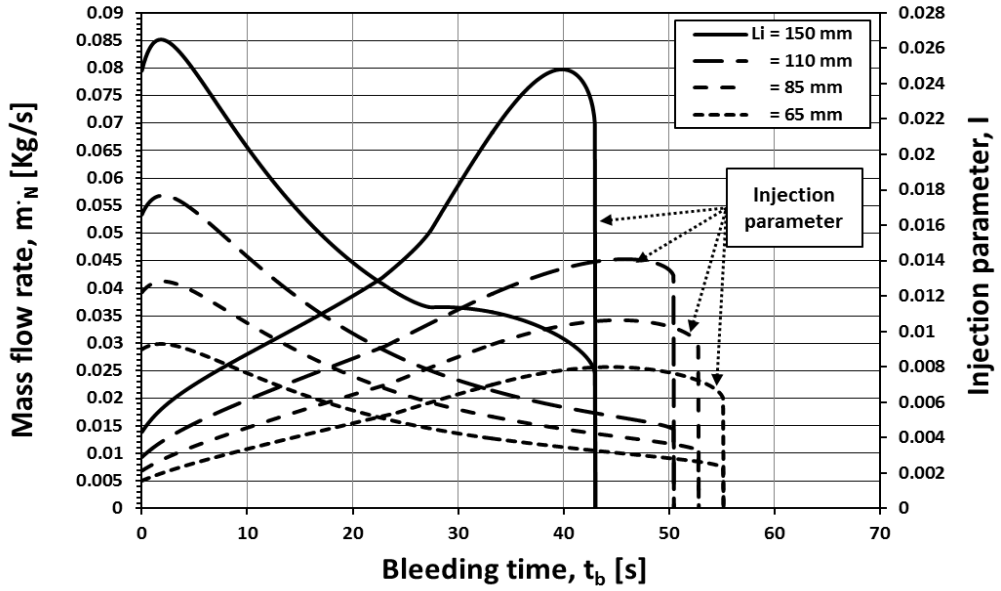

Fig.13. Predicted change of mass flow rate and the injection parameter with bleeding time for different base bleed grain lengths.

Chamber pressure increases with the increase of amount of generated gases from base bleed grain burn and free stream pressure. In the studied cases U_0 and the radial thickness are constants. The increase in the length leads to higher total burn area, mass flow rate and consequently higher chamber pressure as shown in Fig.14. Higher pressure imposes higher burn rate as shown in Fig. 15. This figure plots the burn rate versus bleeding time at different lengths of the grain. It can be noted that there is a reduction in bleeding time with the increase in the length.

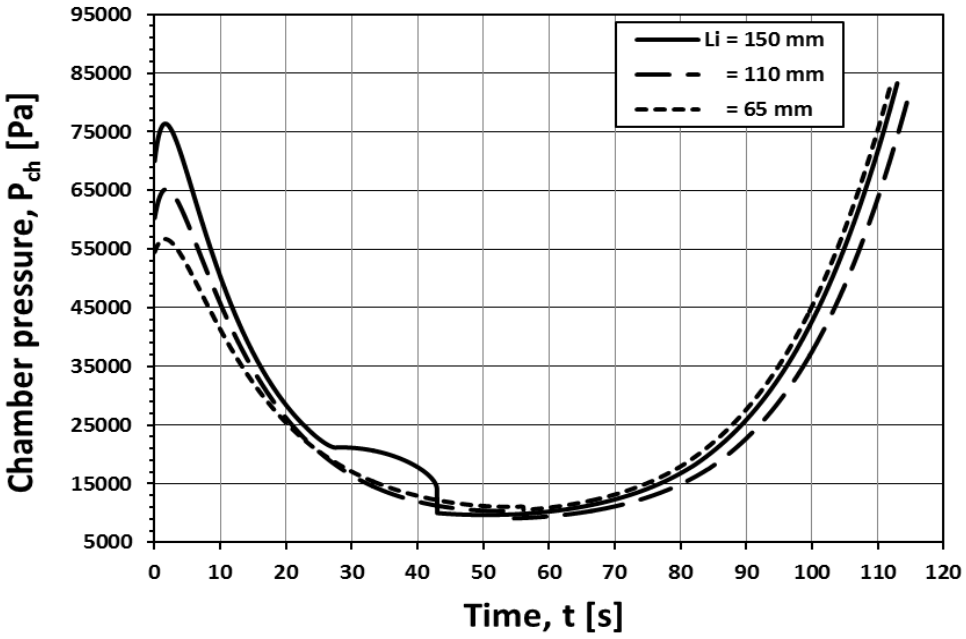

Fig.14. Predicted change of base bleed chamber pressure with time of projectile flight for different base bleed grain lengths.

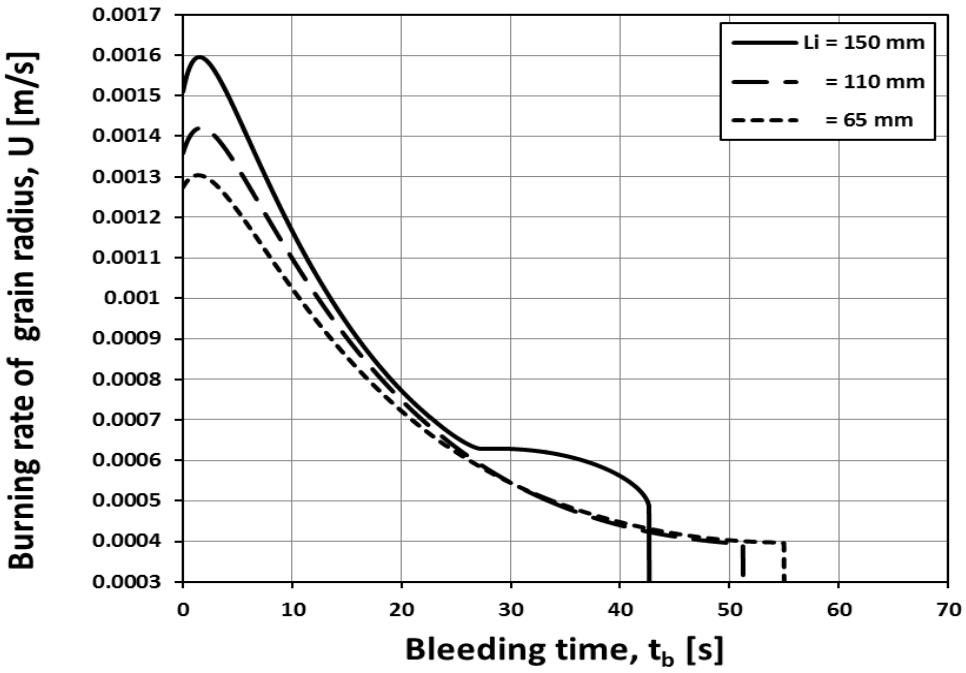

Fig.15. Predicted burn rate of the base bleed grain radius with bleeding time for different base bleed grain lengths.

Figure 16 plots the predicted change of projectile base pressure versus time of projectile flight at different values of the grain length. With the increase in the length from 65 mm to 110 mm, the pressure is higher up to a time equals 18.85 seconds and then the pressure decreases. In case of L_i =150 mm, the pressure increases until the moment when the time equals to 8.9 seconds and then the pressure

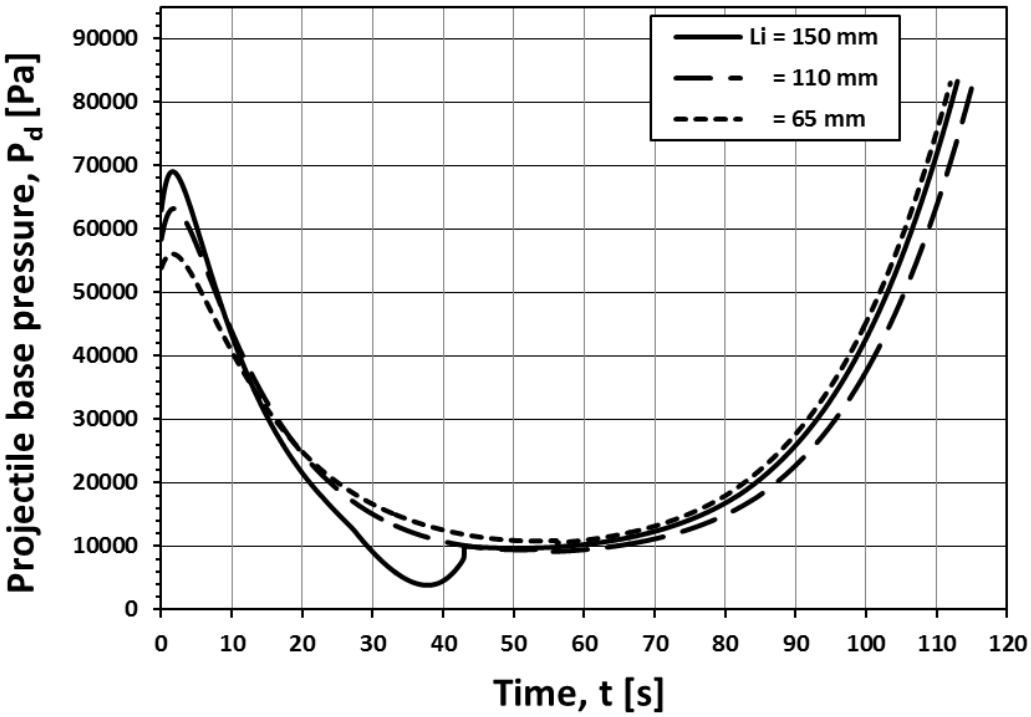

Fig.16. Change of projectile base pressure with time of projectile flight for different base bleed grain lengths

decreases. This occurs under the fact that, the increase in L_i, generates high injection parameter that is higher than the optimum value for longer time during bleeding time and it reaches this high value earlier than in case of the smaller $\mathbf{L_i}$ (see Fig.13). Regarding Refs. [17, 24] which reported that the efficiency of base bleed starts to decrease when the injection parameter is higher than the optimum value this may be attributed to the enough momentum of gases penetrating the wake and consequently the base pressure decreases leading to increase base drag and reduces Mach number as shown in Fig. 11 . If the injection parameter increases more, such as the value reached in case of L_i,= 150 mm, chamber pressure increases leading to high burning rate as shown in Fig. 15 but the base pressure continues to decrease and may reach a value less than the value corresponds to the inert projectile (see Fig. 1) as reached at time equals to 27 seconds. This may be a justification for the decrease of the base pressure, velocity and consequently range seen in Figs. 16, 11 and 9 respectively.

Effect of Base Bleed Grain Inner Radius R_{in}

Figure 17 shows the predicted change of projectile range and base bleed grain bleeding time versus base bleed grain inner radius. The range increases with the increase of the inner radius up to R_{in} = 27mm then it starts to decrease. The bleeding time decreases with the increase of inner radius because the increase in the inner radius decreases the radial thickness of the grain.

Figure 18 depicts the projectile altitude versus the time of flight at specified values of R_{in}. By considering the burning time corresponding to R_{in} = 22 and 32 mm,

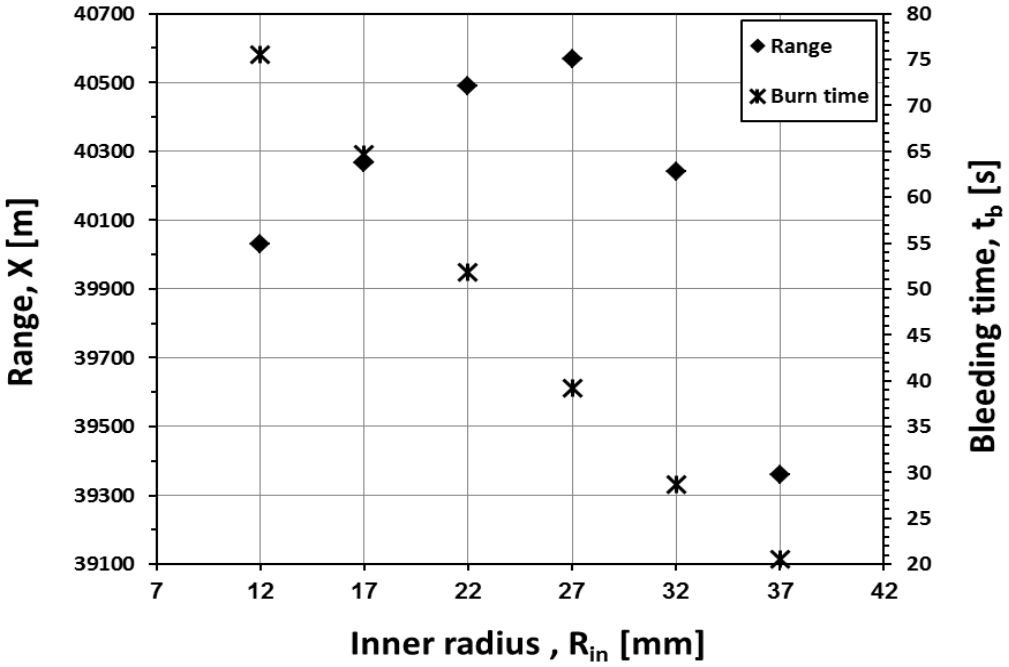

Fig. 17. Predicted projectile range and base bleed grain bleeding time versus inner radius of base bleed grain.

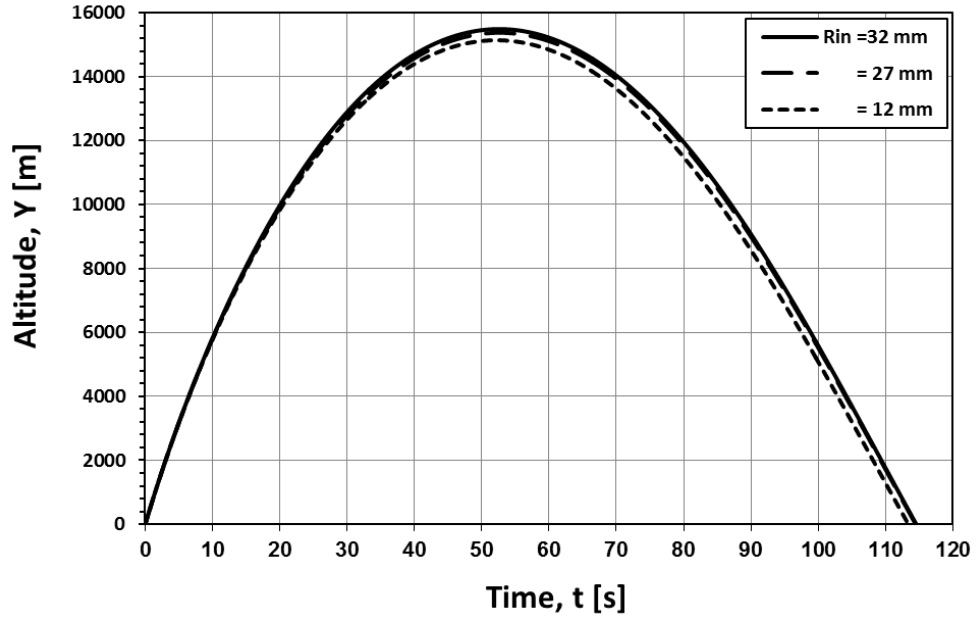

Fig. 18. Change of projectile altitude versus time of flight at different values of base bleed grain inner radius

respectively, cf. Fig. 17 it is clear from the present figure that the bleeding time ends in the ascending part of projectile trajectory.

Figure 19 shows the predicted change of base bleed grain surface areas (cylindrical - slots - total) with bleeding time for selected values of R_{in}. At specified value of R_{in},

the trend of change of cylindrical, slots and total areas is the same as shown previously in Figs. 6 and 12. However the trend of change of the areas at different values of R_{in} is different. The increase of R_{in} leads to an increase in the values of the cylindrical area and a decrease in the slots area (see Fig. 1). Finally the increase in the cylindrical area compensates the decrease in slots area and maintains the total area increasing until the end of burn.

Figure 20 plots the predicted change of mass flow rate and the injection parameter with bleeding time for different inner radii of base bleed grain. It can be seen from the figure, each of mass flow rates or injection parameter take a trend corresponds to the trend of total area. This proves the fact that the base bleed grain provides injection values at small R_{in} values less than the case of larger values of R_{in}. Also, these values are less than the optimum value in the first seconds of burn. But the bleeding time extends for longer time. Therefore, the predicted maximum range increases with the increase of R_{in} up to value 27 mm. The increase in the injection parameter in the first seconds compensates the negative effect of less bleeding time on the range and finally the range increases. For R_{in} >27mm it fails to compensate this negative effect and consequently the range decreases.

For R_{in} = 12 mm the mass flow rate increases again at time > 51.5 seconds which corresponds to the summit of the projectile trajectory. This may be indicated that the bleeding time is continuous in the descending part of projectile trajectory during which the free stream pressure increases with time of flight leading to an increase in the projectile base pressure, chamber pressure which consequently it increases the burn rate and the generated mass flow rate.

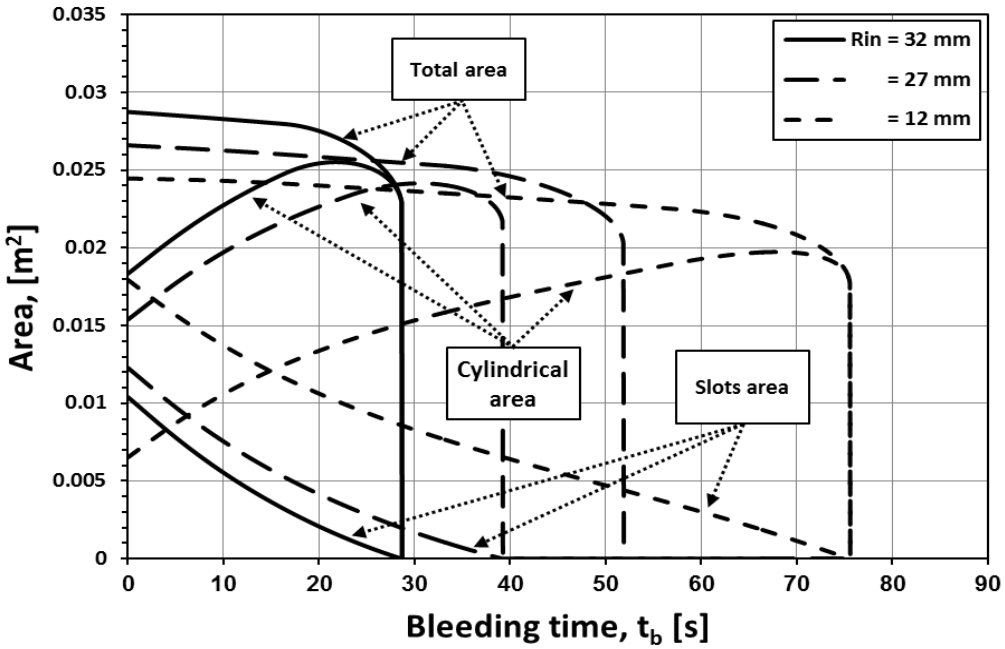

Fig. 19. Change of base bleed grain surface areas (cylindrical – slots - total) v bleeding time at different base bleed grain inner radii.

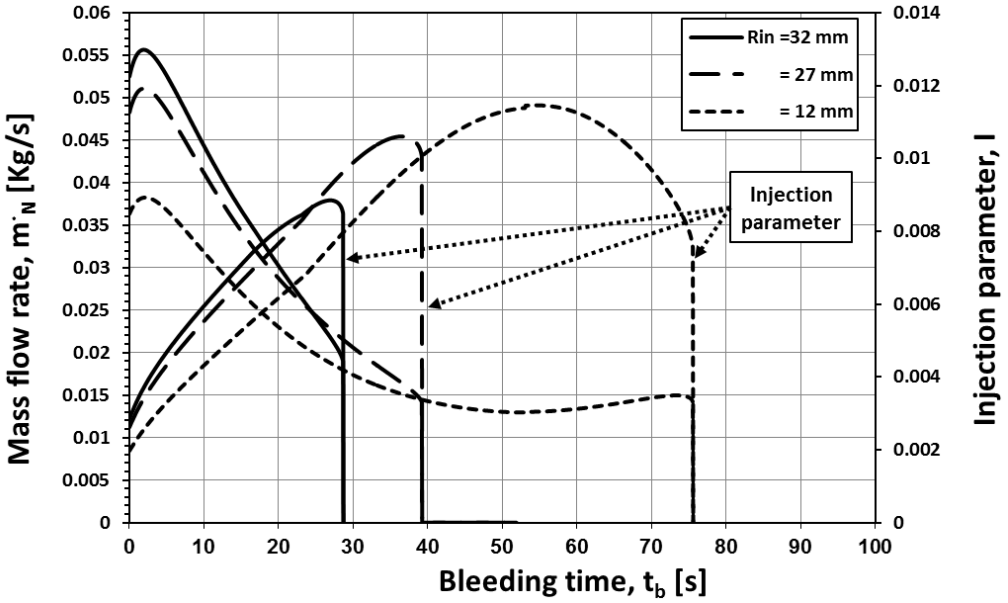

Fig. 20 Change of mass flow rate and the injection parameter versus bleeding time at different inner radii of base bleed grain.

Figure 21 summarizes the effect of the previously studied dimensions (R_{max}, L_i and R_{in}) on range. It is clear that the effect of the R_{in} is the least in both cases, when increasing or decreasing it. The reduction in R_{max} decreases the range with higher percentage than in case of decreasing L_i with the same percentage. However range increases more with the increase in L_i than when increasing R_{max}. Moreover, the effect of reducing R_{max} and L_i on range is higher than in case of increasing it which insures that the original dimensions of the studied base bleed grain are already optimized.

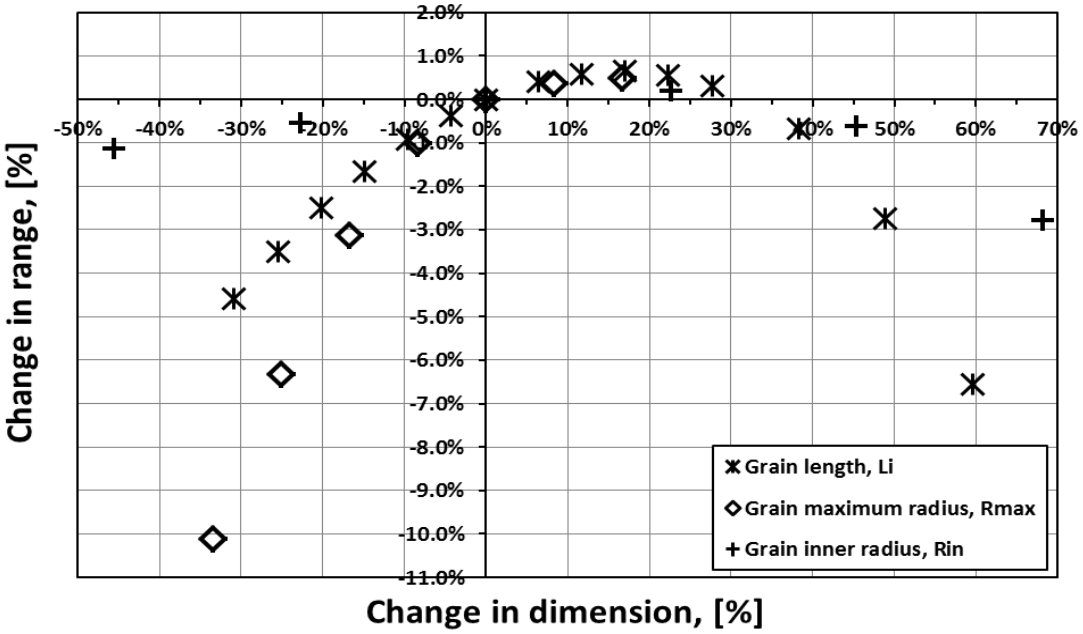

Fig. 21. Predicted effect of base bleed grain dimensions change on range.

Effect of Exit Diameter of Base Bleed Unit D_{exit}

Figure 22 shows the change of projectile range at different exit diameters of base bleed unit and different maximum radii of base bleed grain while the grain length and inner diameter are constant. For each R_{max}, the range increases with the increase in D_{exit} up to a certain value then, no further increase occurs This agrees with the mentioned in [8, 15] which stated that exit diameter has no considerable influence on base pressure when reaches certain size. The exit diameter increases with the increase of R_{max}.

For of R_{max} = 40 mm, no change in the range with the change of D_{exit}. For D_{exit} > 36 mm the increase in R_{max} results in increasing of range. This may be attributed to the fact that with increase in R_{max}, the area exposed to burning increases resulting in more mass flow rate. If the exit area is not large enough to eject the burnt gases, chamber pressure increase and results in larger burning rate which leads to higher injection parameter even more than the optimum in case of larger exit diameter. However it doesn't provide thrust as rocket assistance.

Figure 23 displays the change of mass flow rate and injection parameter versus bleeding time for D_{exit} of 36 and 50 mm, respectively and R_{max}=70mm. For the exit diameters considered, the trends of the injection parameter is not the same. In case of the smaller diameter, higher values of mass flow rate and injection parameter are noticed resulting in less burning time when comparing with the corresponding values of exit diameter = 50 mm. The values of injection parameter in case of exit diameter = 36 mm is much higher from the optimum parameter when comparing with its counterpart values at exit diameter = 50 mm.

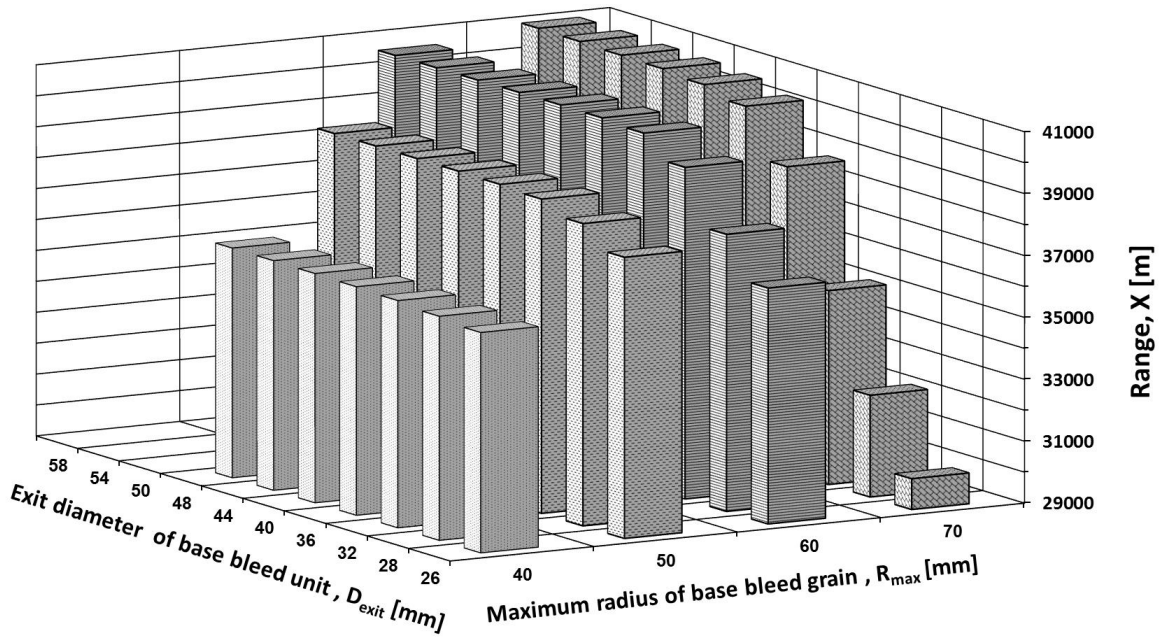

Fig. 22. Change of projectile range at different base bleed exit diameter and different base bleed grain maximum radius

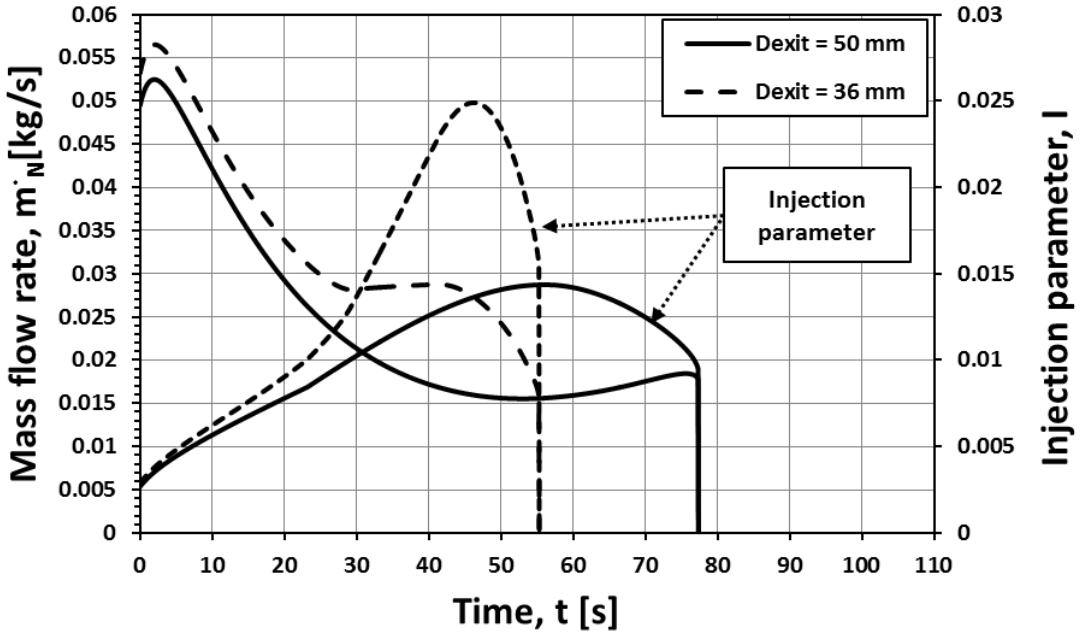

Fig. 23. Change of mass flow rate and the injection parameter versus projectile time of flight at different base bleed exit diameter when R_{max}=70mm.

Figure 24 depicts the change of projectile base pressure with bleeding time. It can be seen that in the first seconds of bleeding time, the base pressure in case of D_{exit}=36mm is higher than the corresponding data in case of D_{exit}=50mm. It is thought that the increase of base pressure in the first seconds is due to the injection parameter value which is close to its optimum value. Once, the injection parameter increases above the optimum value, base pressure decreases dramatically as shown in Fig. 16 and consequently the range decreases.

Figure 25 illustrates the projectile range at different base bleed exit diameter and different base bleed grain length while R_{max} and R_{in} are constants. The trends in the figure are similar to that shown in Fig. 22.

It can be concluded from figures 19 up to 25 that:

i) At the first few seconds of flight smaller exit diameter leads to increase in the mass flow rate because of the trap of more gases inside base bleed chamber which leads to increase the pressure inside, the burning rate and consequently larger injection parameter is obtained when comparing with the injection parameter values corresponding to larger exit diameter.

ii) ii) The increase in mass flow rate during the first few seconds of a supersonic projectile flight overcomes the high free stream velocity resulting in high injection parameter that is closer to the optimum value and maximum drag reduction can be obtained [10, 17, 22].

iii) But in the remaining bleeding time during the ascending part of projectile trajectory, the free stream pressure and velocity decrease and injection parameter increases more than the optimum value especially if the exit diameter is small leading to decrease the base pressure resulting in decreasing in the range.

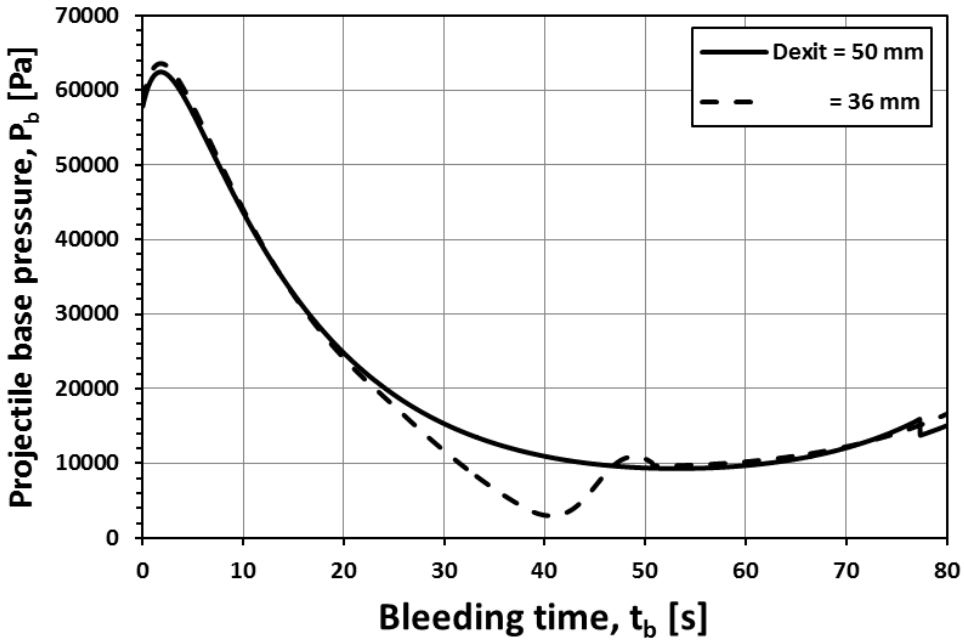

Fig.24. Change of projectile base pressure versus bleeding time at different values of base bleed exit diameter.

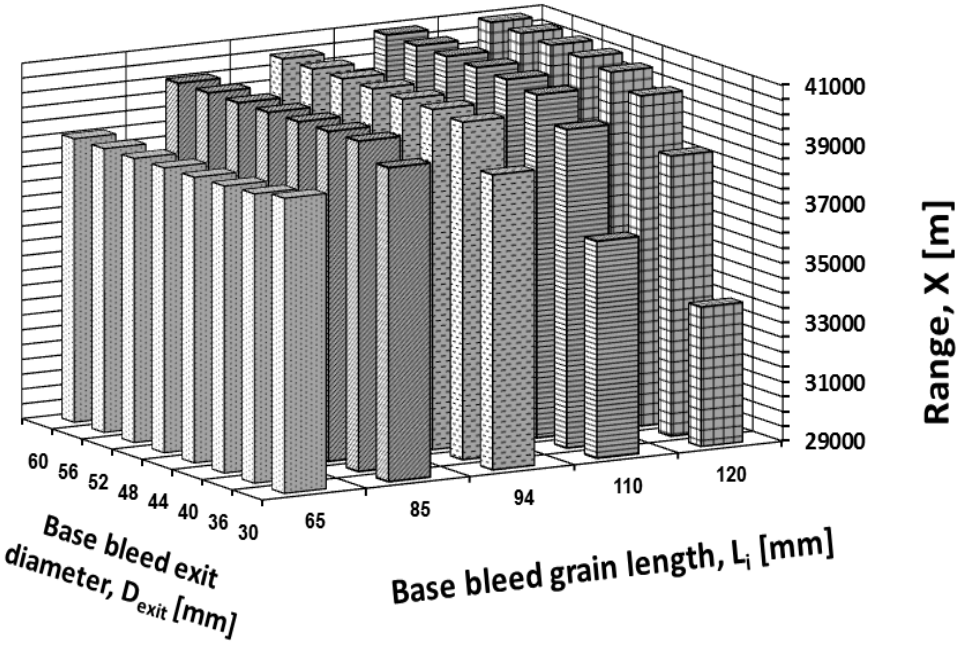

Fig. 25. Projectile maximum range at different base bleed exit diameter and different base bleed grain length

So smaller diameter is more favorable at the first few seconds of a supersonic projectile flight at which higher injection parameter is required. But, during the remaining bleeding time, larger diameter is preferred to increase the mass flow rate preventing the generation of higher injection parameter. Therefore, a new method is proposed which provides a small initial exit diameter which increases gradually as a

function of the chamber pressure until it reaches the required large diameter. This can be achieved by different ways as shown in Fig. 25. The material of the deformable plug could be solid propellant with low burning rate or made of a material that erodes under the effect of the hot gases flow out from base bleed unit such as magnesium.

Figure 26(a) shows schematic drawing for the suggested base bleed unit provided with a plug/ rod. The rod is fixed to the igniter from one of its ends and the other end is located at the base bleed base orifice. The rod is made of erosive material with certain initial diameters and thickness according to the required initial and final exit diameter of base bleed unit. Figure 25(b) shows another suggestion where erosive exit diameter is presented by inserting a plug into the original base orifice. The plug is made of erosive material with initial inner diameter equals to the optimum initial diameter of the base exit and its outer diameter equals to the final exit diameter of base bleed unit.

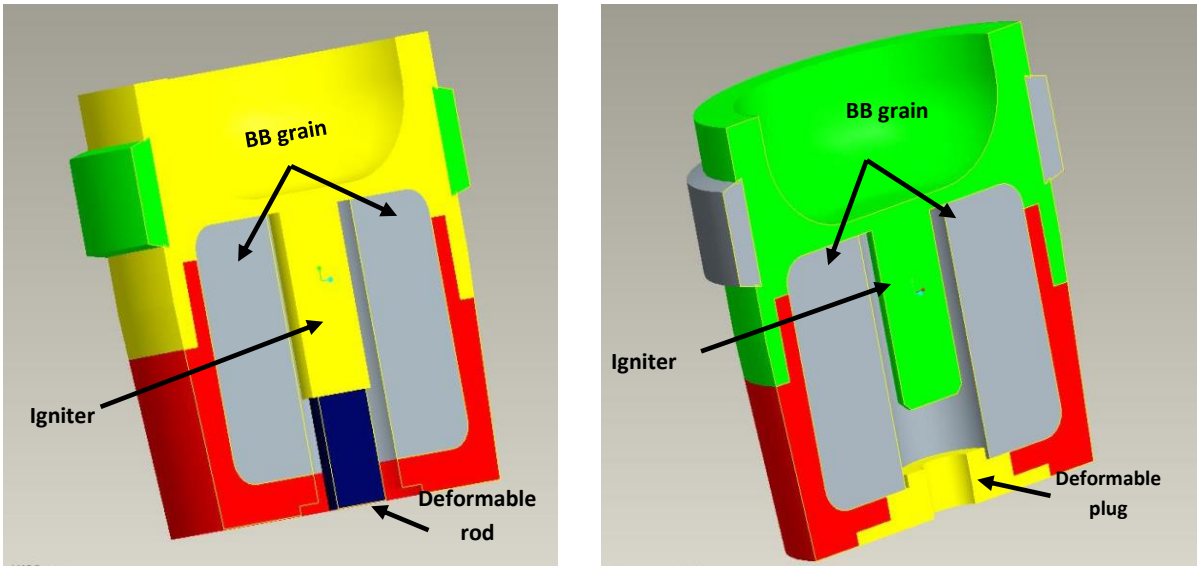

(a) (b)

Fig. 26. Schematic drawing of base bleed unit provided with deformable rod/ plug exit

Figure 27 displays the projectile range and bleeding time in case of a projectile with the original exit diameter = 44 mm, different fixed exit diameter and deformable exit diameter with initial diameter = 22 mm, 24 mm and maximum diameter = 62 mm, 64 mm respectively. It can be seen that the range increases by using deformable exit diameter when comparing with the original diameter or fixed large diameter. For bleeding time, it decreases with the use of deformable exit diameter as the smaller diameter will lead to higher burn rates as discussed before, also bleeding time is less in case of fixed smaller diameter when comparing with the bleeding time of fixed large diameter for the same reason.

Figure 28 illustrates the predicted change of injection parameter with bleeding time at different deformable/fixed base bleed exit diameters. It can be noted that in case of deformable diameter, injection parameter values are higher than the data

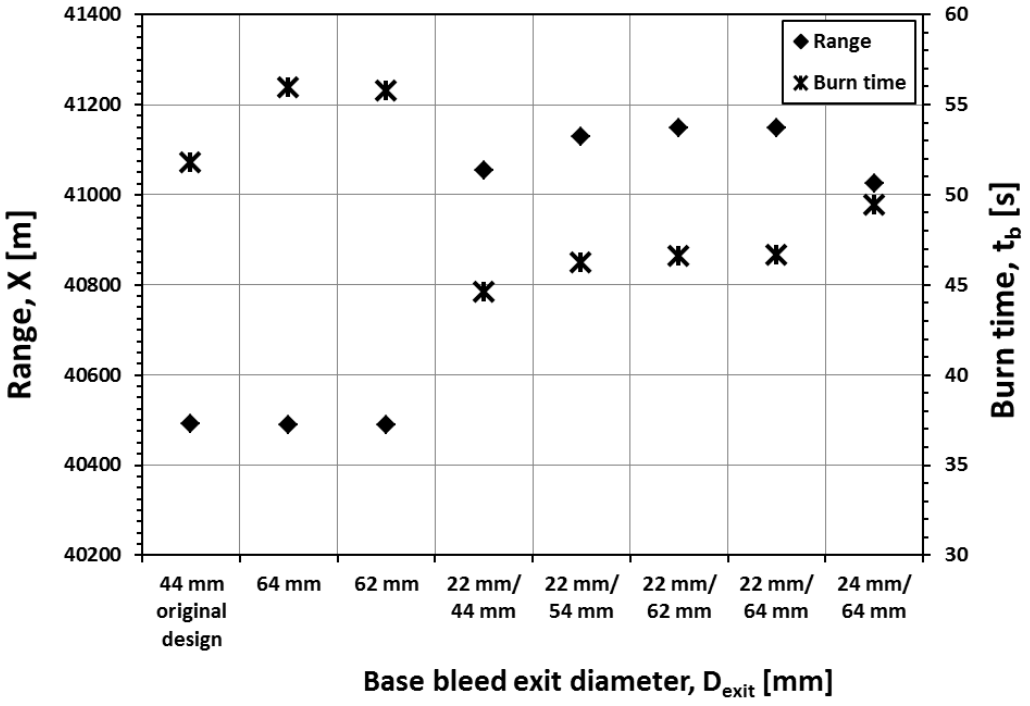

Fig. 27. Projectile maximum range and bleeding time at different deformable/fixed base bleed exit diameter

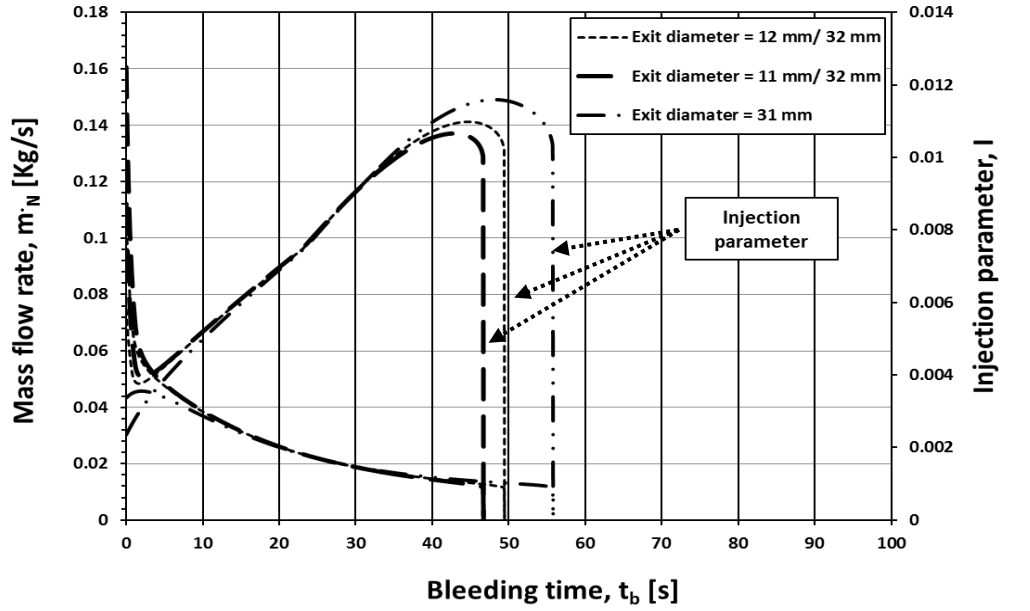

Fig. 28. Predicted change of mass flow rate and the injection parameter wit bleeding time for different (deformable – fixed) base bleed exit diameter**.**

corresponding to fixed diameter during the first few seconds of bleeding time however in the remaining bleeding time, injection parameter values are less and closer to the optimum injection parameter.

CONCLUSION

- When increasing R_{max}, the surface area of the slots, cylindrical area and total area increase. However the cylindrical area for the same radial thickness is the same for all values of R_{max} up to the point when reaching the radius of curved ends (r_s) of the grain.
- The bleeding time increases with the increase of the radial thickness of base bleed grain which equals to ($R_{max} – R_{in}$). However bleeding time decreases with the increase of grain length.
- The increase in L_i results in an increase in both the cylindrical and the slots areas. This leads to the increase of total area up to the end of bleeding time.
- The increase in R_{in} leads to an increase in the values of the cylindrical area and a decrease in the slots area. Finally the increase in the cylindrical area compensates the decrease in slots area and maintains the total area increasing until the end of burn.
- The effect on range when increasing or decreasing R_{in}, is the least when compared with its results with the results of changing R_{max} and L_i.
- The reduction in R_{max} decreases the range with higher percentage than the case of decreasing Li with the same percentage. However range increases more with the increase in Li than when increasing R_{max}.
- The effect of reducing R_{max} and L_i on range is higher than in case of increasing these dimensions which insures that the original dimensions of the studied base bleed grain are already optimized.
- Smaller exit diameter results in generating larger mass flow rate, less burn rate and consequently higher injection parameter when comparing with the values corresponding to larger exit diameter.
- Smaller diameter is more favorable in the first few seconds of projectile flight since higher injection parameter is required but, at the remaining bleeding time, larger diameter is required to allow larger mass flow rate and prevent the generation of higher injection parameter.
- Optimization of base bleed grain dimensions is a combination of optimization of its different dimensions besides exit diameter as well as the grain combustion parameters.
- A new method is presented which is thought to provide a smaller initial small exit diameter that will increase gradually as function of the chamber pressure reaching maximum exit diameter. The study shows that the range increases with 1.7 % when applying this method compared with the range of a base bleed projectile provided with a fixed exit diameter.

REFERENCES

[1] K. Anderson, N. E. Gunners and R. Hellgren, "Swedish Base Bleed - Increasing the Range of Artillery Projectiles through Base Flow", Propellants and Explosives I, 69-73 (1976).

[2] Nils E. Gurnners, K. Andersson and R. Hellgren, "Base-Bleed Systems for Gun Projectiles", Aeronautics and Astronautics Progress, Vol. 16, No. 1, pp. 537-561 (1987).

[3] Nils-Erik, K. Andersson and Y. Nilson "Testing of Parts and Complete Units of the Swedish Base Bleed System", First International Symposium on Special Topics in Chemical Propulsion, Athens, Greece, 23-25 November (1988).

[4] L. D. Kayser, J. D. Kuzan and D. N. Vazquez, "Flight Testing for a 155mm Base Burn Projectile", (AD-A222 562) April (1990).

[5] L. D. Kayser, J. D. Kuzan and D. N. Vazquez, "In-Flight Pressure Measurements on Several 155mm, M864 Base Burn Projectiles", AD-A232 225, January (1991).

[6] J.E. Bowman and W.A. Clayden, "Cylinderical Afterbodies in Supersonic Flow with Gas Ejection," AIAA Journal, Vol. 5, No. 8 : pp. 1524-1525 (1967).

[7] W.A. Clayden and J.E. Bowman, "Cylindrical Afterbodies at M=2 with Hot Gas Ejection", AIAA Journal, Vol. 6, No. 12, pp 2429-2431 (1968).

[8] Z. Ding, S. Chen, Y. Liu, R. Luo and J. Li, "Wind Tunnel Study of Aerodynamics Characteristics of Base Combustion" , Journal of Propulsion and Power, Vol. 8, No. 3, pp. 630-634 (1992).

[9] T. Mathur and J. C. Button, "Base-Bleed Experiments with a Cylindrical Afterbody in Supersonic Flow" Journal of Spacecraft and Rockets, Vol. 33, No. 1, pp. 30-37 (1996).

[10] S. Jaramaz and M Injac, "Effect of grain characteristics on range of artillary projectiles with base bleed", First International Symposium on Special Topics in Chemical Propulsion, Athens, Greece, 23-25 November (1988).

[11] J. Danbergand, "Analysis of the Flight Performance of the 155 mm M864 Base Burn Projectile", Technical Report BRL-TR-3083, April (1990).

[12] J. Danberg and C. Nietudicz, "Predicted Flight Performance of Base Bleed Projectile", 26th Joint Propulsion Conference, Florida, USA, 16-18 July (1990), (AIAA 90-2069).

[13] R. F. Lieske and J. E. Danbergt, "Modified Point Mass Trajectory Simulation for Base-Burn Projectiles", Astrodynamics Conference, USA, 1992, (AIAA-92-4641).

[14] J. - S. Hwang and C-K Kim, "Structure and Ballistic Properties of K307 Base Bleed Projectile", 16th Int. Sympo. on Ballistics, California, USA, 23-27 September (1996).

[15] A.Z. Ibrahim, "Ballistic Performance of Base Bleed Unit", M. Sc. Thesis, MTC (2000).

[16] Z. Ling-Ke, Z. Yan-Huang, Y. Yong-Gang and Z. Wei, "Studying on Firing Range of Base Bleed Projectile Caused by Inconsistent Base Bleed Unit Working", 25th Int. Sympo. on Ballistics, Beijing, China, 17-21 May (2010).

[17] H. A. Abou-Elela, A. Z. Ibrahim, O. K. Mahmoud and O. E. Abdel-Hamid, "Ballistic Analysis of a Projectile Provided with Base Bleed Unit", 15th International Confrenceon Aerospace Scienses & Aviation Technology,ASAT-15, Egypt, 28 -30 May (2013).

[18] J. – Y. Choi, E. Shin and C-K Kim, "Numerical Study of Base-Bleed Projectile with External Combustion", 41st AIAA/ASME/SAE/ASEE Joint Propulsion Conference & Exhibit, Arizona, USA, 10 - 13 July (2005).

[19] H. Bournot, E. Daniel and R. Cayzac, "Improvements of the Base Bleed Effect Using Reactive Particles", International Journal of Thermal Sciences, 45, pp. 1052–1065 (2006).

[20] Y. – K. Lee, H. – D. Kim and S. Raghunathan, "Optimization of Mass Bleed for Base-Drag Reduction" AIAA Journal, Vol. 45, No. 7 pp. 1472-1477 (2007).

[21] N. Hubberud and I. J. Ye, "Extended Range of 155mm Projectile Using an Improved Base Bleed Unit. Simulation and Evaluation", 26th Int. Sympo. on Ballistics, Florida, USA, 12-16 September (2011).

[22] K. Andersson, "Different Means to Reach Long Range > 65 Km, for Future 155mm Artillery Systems. Possibilities and Limitation", 17th Int. Sympo. on Ballistics, Midrand, South Africa, 23-27 March (1998).

[23] A. Davenas, "Solid Rocket Propulsion Technology", Pergamon Press Ltd., England, pp. 350 (1993).

[24] Mathur, Tarun, "An Experimental Investigation of the Effects of Base Bleed in Axisymmetric Supersonic Flow", (Ph.D thesis, university of Illinois (1996).